CHOKED TWO-PHASE FLOW WITH ACCOUNT OF DISCHARGE LINE EFFECTS

A.G. Venetsanos
Environmental Research Laboratory, National Centre for Scientific Research "Demokritos",
15310 Aghia Paraskevi, Attikis, Greece, venets@ipta.demokritos.gr

Keywords: Liquefied Hydrogen, two-phase flow, choked flow, Fanno flow

Abstract

An engineering tool is presented to predict steady state two-phase choked flow through a discharge line with variable cross section with account of friction and without wall heat transfer. The tool is able to predict the distribution of all relevant physical quantities along the discharge line. Choked flow is calculated using the possible-impossible flow algorithm, implemented in a way to account for possible density discontinuities along the line. Physical properties are calculated using the Helmholtz Free Energy formulation. The tool is verified against previous experiments with water and evaluated against previous experiments with cryogenic two-phase hydrogen.

1 NOMENCLATURE

Latin symbol	Physical meaning	Units
A	Cross sectional area	m^2
D	Hydraulic diameter	m
f	Darcy friction coefficient	-
w	Velocity	m/s
h	Enthalpy	J/kg
v	Specific volume	m^3/kg
G	Mass flux	$kg/m^2/s$
P	Pressure	Pa
s	Entropy	J/kg/K
T	Temperature	K
x	Vapor quality (mass fraction)	-
y	Mass fraction of the total stable phase (vapour + liquid)	-
z	Axial distance from discharge line start	m

Greek symbol	Physical meaning	Units
α	Void fraction	-
θ	Thermal relaxation time of HRM model	s
μ	Dynamic viscosity	Pa s
ρ	Density	kg/m^3

Subscript	Physical meaning
0	Stagnation conditions
1	Upstream location
2	Downstream location
b	Back pressure
CR	Critical thermodynamic point
LM	Liquid in metastable condition
LS	Liquid saturated
onset	Nucleation onset

VS	Vapor saturated
SAT	Saturated conditions
HEM	Homogeneous Equilibrium model

2 INTRODUCTION

Before hydrogen is established as energy carrier and extensively used in the society, issues regarding the safety of hydrogen applications must be thoroughly examined using all means of scientific analysis (theory, experiments and simulations) and risk assessment must be applied to demonstrate that associated risks are below acceptable levels.

In such a process source estimation in case of a potential accident, is the first step of any safety analysis and of primary importance for the final results. Therefore, reliably accurate source estimation is a primary requirement / target and this holds not only for hydrogen applications but generally for all applications that may pose risks to society, such as the nuclear industry for example.

In the case of onsite hydrogen storage a potential accident could be the full bore (or partial) rupture of the transfer line from the tank to other parts of the installation. The effects of the line itself, i.e. from the tank to the break location (pipe friction, pipe varying diameter, wall heat transfer) should be adequately investigated. It should be noted that line effects do not concern only accidental situations, but also installation design, e.g. for transferring hydrogen from a tanker to the storage tank.

The problem of discharge line effects concerns all kinds of hydrogen storage (cryogenic or not), but is far more complex when two-phase flow is possible within the line, due to the difficulty and complexity in modeling nucleation and flashing processes.

Critical two-phase flow modeling has been the subject of many investigations in the past [1, 2, 3, 4, 5, 6]. Modeling approaches for flashing and nucleation were categorized in [5] by considering at most four consecutive zones along the discharge line direction: a) sub-cooled liquid (if stagnation conditions are sub-cooled) b) superheated liquid (metastable) c) non-equilibrium nucleation and d) equilibrium nucleation.

In the present work we focus on the classical Homogeneous Equilibrium Model (HEM), and two well-known homogeneous non-equilibrium relaxation models: the Delayed Equilibrium Model (DEM) [7, 8] and the Homogeneous Relaxation Model (HRM) [9, 10]. Main scope of the work is to implement these models in an engineering computational tool (not CFD) and perform an evaluation of their performance compared to existing (or new) data for water and hydrogen if possible.

Two additional requirements were set herein regarding the computational procedure: a) to be able to treat discontinuities, which are present e.g. for HEM when the liquid saturation line is crossed, see [6] and b) to be able to calculate the flow and conditions along the discharge line, beyond the critical location. These requirements are not satisfied with the choked two-phase flow procedure presented in [7], which is based on solving the respective conservation equations in characteristic form.

3 MATHEMATICAL FORMULATION

3.1 Basic Conservation equations

In the work we are limiting ourselves (as a first step) to steady state, adiabatic conditions and neglect any gravity effects. The conservation equation of mass, momentum and energy along the discharge line are given below, see also [7].

Mass conservation:

$$d(GA) = 0\,, \quad G \equiv \rho w \tag{1}$$

Momentum conservation:

$$dP = -vG^2\left(\frac{dv}{v} - \frac{dA}{A} + \frac{fdz}{2D}\right) \tag{2}$$

Energy conservation:

$$d\left(h + \frac{1}{2}(Gv)^2\right) = 0 \tag{3}$$

Darcy friction coefficient:

$$\sqrt{f} = \frac{1}{0.87\ln\left(\mathrm{Re}\sqrt{f}\right) - 0.8}, \quad \mathrm{Re} \equiv \frac{GD}{\mu} \tag{4}$$

3.2 Single phase flow

Taking into account the physical properties dependencies, the system of eq. (1)-(3) with given upstream conditions is closed with three downstream unknowns: (P, T, G).

3.3 Two-phase flow with Homogeneous Equilibrium Model (HEM)

In the HEM model, the mixture is composed of saturated vapor and saturated liquid:

$$v = xv_{VS} + (1-x)v_{LS} \tag{5}$$

$$h = xh_{VS} + (1-x)h_{LS} \tag{6}$$

Mixture viscosity is calculated based on the following relation:

$$\frac{v}{\mu} = \frac{xv_{VS}}{\mu_{VS}} + \frac{(1-x)v_{LS}}{\mu_{LS}} \tag{7}$$

Taking into account the mixture and phase physical properties dependencies, the system of eq. (1)-(3) with given upstream conditions is closed with three downstream unknowns: (P, x, G).

3.4 Two-phase flow with Homogeneous Relaxation Model (HRM)

In the HRM model, the mixture is composed of saturated vapor and metastable liquid (superheated). Mixture physical properties are then given by:

$$v = xv_{VS} + (1-x)v_{LM} \tag{8}$$

$$h = xh_{VS} + (1-x)h_{LM} \tag{9}$$

HRM model uses the following equation for vapor generation along the pipe:

$$G\frac{dx}{dz} = \rho\frac{\bar{x} - x}{\vartheta}, \text{ where: } \bar{x} = \frac{h - h_{SL}}{h_{SV} - h_{SL}} \tag{10}$$

For water the thermal relaxation time is given by:

$$\vartheta = \begin{cases} 6.51\times10^{-4}\, a^{-0.257}\left(\dfrac{P_{SAT}(T_0)-P}{P_{SAT}(T_0)}\right)^{-2.24}, & \text{if } P \le 10bar \\ 3.84\times10^{-7}\, a^{-0.54}\left(\dfrac{P_{SAT}(T_0)-P}{P_{CR}-P_{SAT}(T_0)}\right)^{-1.76}, & \text{if } P > 10bar \end{cases} \tag{11}$$

The mixture void fraction is defined by the equation below, which is a general definition valid for all models.

$$\alpha \equiv x\frac{v_{VS}}{v} \tag{12}$$

Taking into account the mixture and phase physical properties dependencies, and the thermal relaxation time dependency, the system of eq. (1)-(3) together with eq. (10), with given upstream conditions is closed with four downstream unknowns: (P, x, G, T_{LM}).

3.5 Two-phase flow with Delayed Equilibrium Model (DEM)

In the Delayed Equilibrium Model, the mixture is composed actually of three phases: saturated vapor, saturated liquid and metastable liquid. Mixture physical properties are then given by:

$$v = xv_{VS} + (y-x)v_{LS} + (1-y)v_{LM} \tag{13}$$

$$h = xh_{VS} + (y-x)h_{LS} + (1-y)h_{LM} \tag{14}$$

DEM model uses the following equation for total stable phase generation along the pipe:

$$\frac{dy}{dz} = \left(C_1\frac{4}{D} + C_2\right)(1-y)\left(\frac{P_{SAT}(T_{LM})-P}{P_{CR}-P_{SAT}(T_{LM})}\right)^{C_3} \tag{15}$$

For water the coefficients are:

$$C_1 = 0.008390,\ C_2 = 0.633691,\ C_3 = 0.228127 \tag{16}$$

The model also accounts for a vaporization delay, by application of eq. (15) only when pressure becomes lower than the onset pressure for nucleation below. If the pressure is higher than the nucleation onset pressure the model assumes zero total stable phase mass fraction (y = 0).

$$P_{onset} = 0.95P_{SAT}(T_0) \tag{17}$$

Regarding the metastable liquid temperature, the model assumes that the metastable phase undergoes an isentropic expansion:

$$s_{LM} = s_{LM}(T_{LM}, P) = ct \tag{18}$$

Taking into account the mixture and phase physical properties dependencies, the system of eq. (1)-(3) together with eq. (15) and eq. (18), with given upstream conditions is closed with five downstream unknowns: (P, x, y, G, T_{LM}).

3.6 Phase physical properties

In the present work single phase physical properties were calculated using accurate equations of state (EoS) explicit in terms of Helmholtz Free Energy, see [11, 12]. The developed numerical code though was structured in a way to easily incorporate other simpler EoS.

For single phase flow we have:

$$v = v(T,P), \quad h = h(T,P) \tag{19}$$

For two-phase flow, phases share the same pressure, but different temperatures. Vapor phase is saturated. Liquid phase can be saturated and/or metastable.

$$v_{VS} = v_{VS}(T_{SAT},P), \quad h_{VS} = h_{VS}(T_{SAT},P) \tag{20}$$

$$v_{LS} = v_{LS}(T_{SAT},P), \quad h_{LS} = h_{LS}(T_{SAT},P) \tag{21}$$

$$T_{SAT} = T_{SAT}(P) \tag{22}$$

$$v_{LM} = v_{LM}(T_{LM},P), \quad h_{LM} = h_{LM}(T_{LM},P) \tag{23}$$

4 NUMERICAL FORMULATION

4.1 Discretization strategy

A discharge line is grid is formed, by defining an adequate number of stations along the discharge line. Conservation equations (1)-(3) as well as (10) and (15) are discretized along a discharge line element of step Δz, located between two consecutive line stations. Mass and energy conservation equations (1) and (3) are directly integrated on this element, but momentum equation (2) cannot be directly integrated. In the second case, linear interpolation between adjacent line stations is used to calculate the specific volume, mass flux, line diameter and friction coefficient entering in eq. (2). In the case of equations (10) and (15), the left hand side derivatives are calculated using simple Euler scheme, while the right hand side terms are evaluated only at the downstream location.

4.2 Downstream advancement Algorithm

The solution procedure to calculate downstream conditions for given upstream conditions is iterative over the downstream pressure in the range $[P_b,P_1]$. In all models downstream mass flux is calculated first from eq. (1).

In the case of single phase flow, temperature is calculated iteratively from the energy eq. (3). In the case of HEM model, vapor quality is found from eq. (3) analytically, after substituting the mixture relations.

In the case of non-equilibrium models HRM and DEM calculations are more complex. In HRM model the energy eq. (3) is coupled with the vapor phase formation equation (10) and must be solved by iterations simultaneously. Iterations here are performed over the metastable liquid temperature. In DEM model, the metastable liquid temperature is obtained first from eq. (18). Then the total stable phase mass fraction is obtained from eq. (15) and then the vapor quality is obtained from the energy eq. (3).

In all models downstream pressure iterations end if momentum eq. (2) is also satisfied. If no simultaneous solution of the whole system of equations is found, then this physically means that the flow, as defined by the upstream conditions, is impossible to propagate downstream.

4.3 Possible-Impossible-Flow Algorithm for choked flow calculation

Choked flow is calculated using the Possible-Impossible-Flow (PIF) algorithm. This algorithm determines the choked flow rate as the maximum of the possible and minimum of the impossible flow rates through the discharge line.

The procedure adopted in this work is iterative over the pressure at the beginning of the discharge line (z = 0). Conditions (and flow rate) at this location are calculated by performing an isentropic expansion from the known stagnation conditions inside the tank. The two-phase model applied in this work, for this isentropic expansion is HEM. Next the downstream advancement algorithm is applied till either a) the pipe end is reached, which physically means that we have a possible flow, or b) an "impossible" condition is reached somewhere along the line. In case-a, the pressure at the beginning of the discharge line is decreased to produce a higher flow rate (isentropic expansion from stagnation to this decreased pressure will increase the flow rate). In case-b the pressure at the beginning of the discharge line is increased to produce a lower flow rate.

5 RESULTS AND DISCUSSION

5.1 Super Moby Dick water experiments (1980)

Preliminary validation work was performed against experimental data from the Super Moby Dick experiments with water [13], for which detailed information has been measured and reported regarding pressure and void fraction distribution along the discharge line. The experiment selected has a stagnation state with pressure 20 bar and temperature 212.3 C.

Figure 1 shows the modeled discharge line geometry, comprised of a) a smooth convergent initial part of length 10 cm, in which the diameter changes from 6.67 cm to 2 cm, followed by b) a constant diameter part of length 36.3 cm and ending with c) a conical divergent diameter part of length 10 cm, in which the diameter increases from 2 cm to 3.24 cm (7° semi-angle). As shown in the figure by solid circles, the discharge line was discretized using a grid of total 84 axial stations, 61 for the converging part, 18 for the constant part and 5 for the linear part. Based on theory, choked conditions are expected at or very near to the end of the constant diameter part.

Figure 2 below shows the predicted pressure, void fraction and axial velocity evolution along the discharge line using all three models HEM, HRM and DEM, compared against the experimental data. The difference in void fraction predictions trend between HEM and the non-equilibrium models is remarkable. HEM model does not account for any delay in vaporization. As a result the HEM predicted void fraction increases very fast within the initial convergent part in contradiction to the experimental behavior. The predicted void fraction evolution trend with HRM and DEM is consistent with the experimental evidence. For the present experiment DEM seems to produce the best results compared to the experimental void fraction data. The mass flow rates predicted by HEM, HRM and DEM for this experiment are 3.33, 3.56 and 5.19 kg /s respectively. Experimental mass flow rates were not reported in [7]. Account of non-equilibrium increases the flow rate as expected. The HEM model, despite its inability to predict correctly the void fraction distribution manages to predict a mass flow rate close enough to HRM.

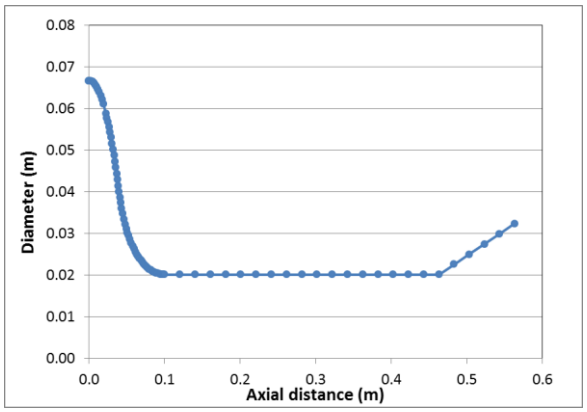

Figure 1. Pipe diameter variation along the discharge line for the Super Moby Dick experiments. Solid circles show the grid locations.

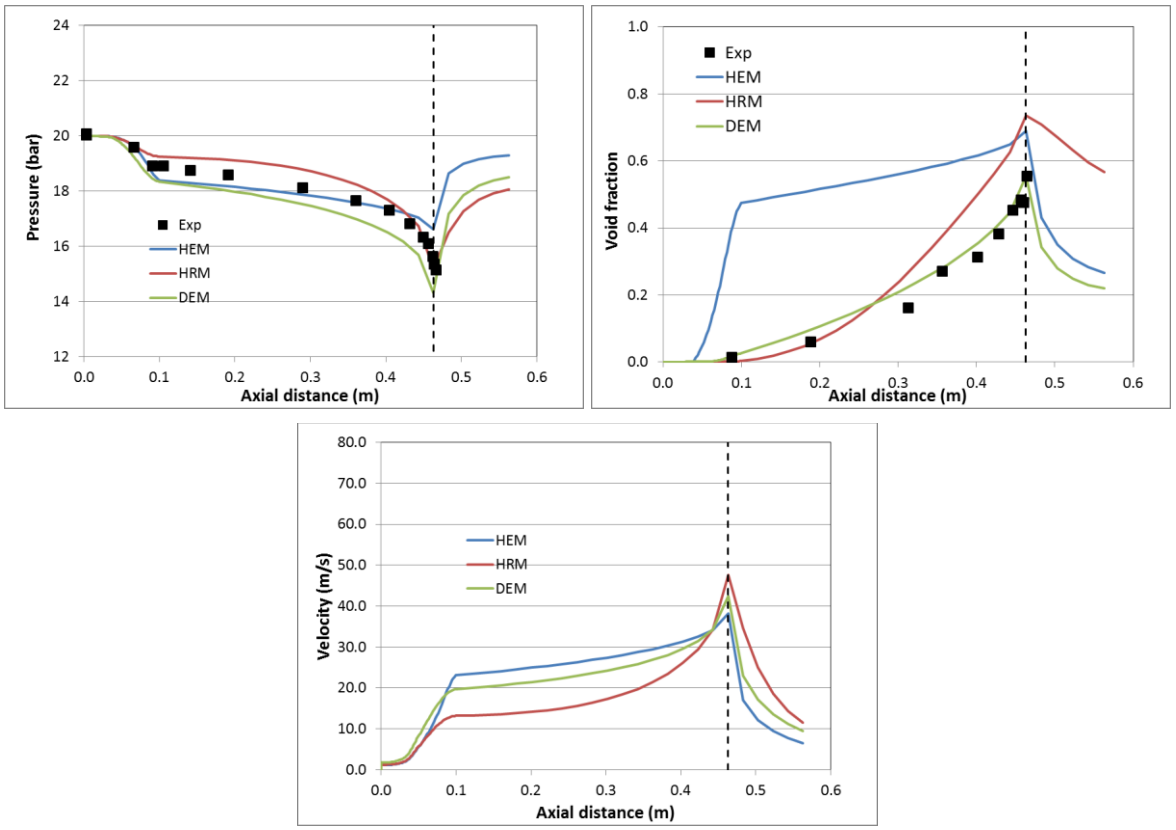

Figure 2. Predicted evolution along discharge line of pressure (top left) and void fraction (top right) and axial velocity (bottom) for liquid water at stagnation state 20bar, 212.3 C, compared against the Super Moby Dick experimental data. Vertical dotted line shows location of critical section.

5.2 NASA LH2 experiments (1984)

In 1984 large scale liquefied hydrogen spill experiments were performed by NASA [14]. According to this reference, the discharge line in the tests performed consisted of a) an initial 10.2 cm diameter part, which extended from an access hatch in the top of the LH2 Dewar to a location close to the bottom of the Dewar, b) a valve that provided a transition from 10.2 cm to an internal diameter of 15.2 cm and c) an approx. 30 m long foam-insulated line of 15.2 cm constant internal diameter. To conduct a spill, gaseous helium was used to pressurize the spill Dewar to as high as 6.9 bar. For Test-6, 5.7 m^3 of LH2 were released in 35 s, giving an average mass flow rate of 11.5 kg/s.

It should be noted regarding the NASA experiments that the first part of the discharge line had a smaller diameter than the last 30 m part and therefore based on theory choking would occur at or near the end of this first part. Unfortunately no information was reported on the length of this first part.

For the simulations stagnation conditions inside the LH2 tank were assumed to be, 6.9 bar pressure and corresponding saturated temperature of 29.07 K. Regarding the length of the first discharge line part, it was estimated from figure 1 of reference [14], to be approximately 10 m, accounting for the fact that this first part should also have an extension within the Dewar itself. Regarding the diameter transition part this was assumed to occur within zero line length (i.e. discontinuity) and in this case isentropic expansion was used to connect the two diameters. The 30 m long line was also extended by 2 m to account for the vertical part just before the line exit, see [14].

Figure 3 below shows the predicted pressure and void fraction evolution along the discharge line, using HEM model, while Figure 4 shows the predicted Mach number and vapor quality evolution. Solid circles denote the calculation stations along the line (22 stations in the 10 m initial part and 37 stations in the last 32 m part), which were distributed with higher density close to the expected choked conditions location (end of 10m section). Predictions show that choking occurred at this location. The existence of the sudden diameter transition resulted in large sudden changes in pressure and void fraction, as shown. Pressure predictions show that the flow exiting the discharge line is at a pressure above atmospheric. Predicted mass flow rate was 22.8 kg/s, i.e. approximately twice the experimentally reported. This overestimation could be due to unknown extra resistances and/or heat transfer effects, which were not accounted herein. Finally, it should be noted that any application of non-equilibrium two-phase modeling or pure liquid flow modeling (Bernoulli) would lead to mass flow rates even higher than those predicted with HEM.

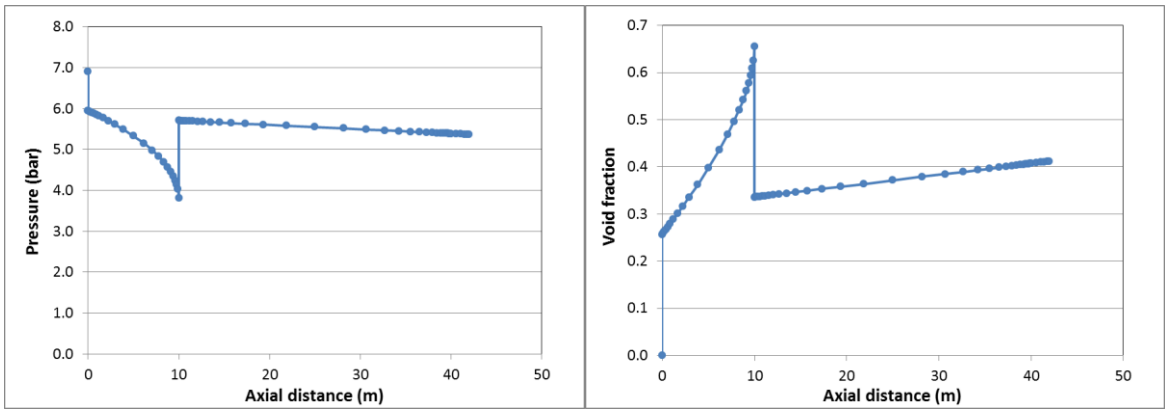

Figure 3. Predicted evolution along discharge line of pressure (left) and void fraction (right), for NASA-1984 tests. Solid circles show the grid locations

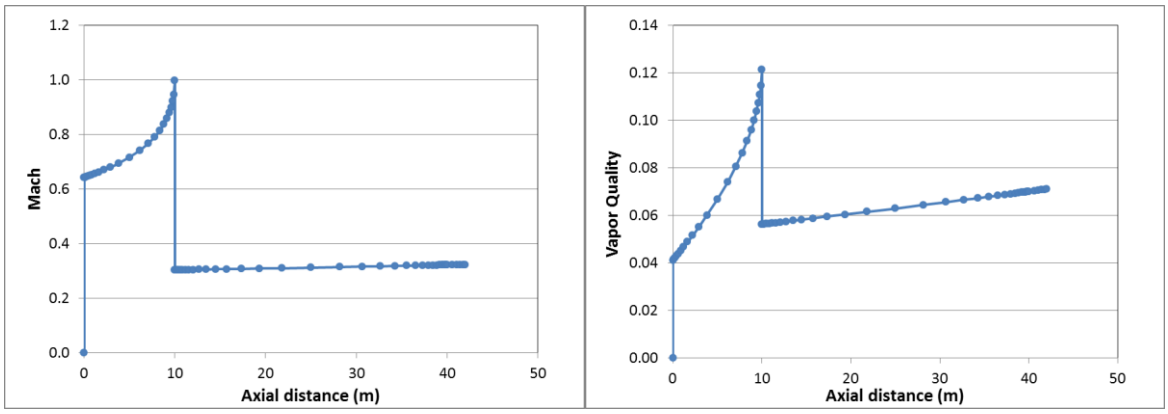

Figure 4. Predicted evolution along discharge line of Mach (left) and vapor quality (right), for NASA-1984 tests. Solid circles show the grid locations

5.3 HSL-HSE LH2 experiments (2010)

In the LH2 release experiments performed by HSL [15] in 2010, the discharge line comprised of 20 m of 1" nominal bore vacuum insulated hose, followed by 1.6 m of un-insulated pipe of the same nominal bore. A nozzle diameter of 2.63 mm was reported. To conduct a spill, hydrogen tanker pressure was raised to 2 bar using a heat exchanger. Volumetric flow rate was reported to be 60 L/min corresponding to a mass flow rate of approximately 0.07 kg/s.

For the simulations stagnation conditions inside the LH2 tank were assumed to be, 2.0 bar pressure and corresponding saturated temperature of 22.91 K. The entire line was assumed to have a diameter of 26.3 mm.

Figure 5 below shows the predicted pressure and void fraction evolution along the discharge line using HEM model. Figure 6 shows the predicted Mach number and vapor quality evolution. Solid circles denote the calculation stations along the line (34 stations distributed with higher density close to the line beginning and end. Predictions show that flow was expanded at the discharge line exit, with Mach number approximately 0.7 at this location. Predicted mass flow rate was 0.42 kg/s, i.e. approximately 6 times the experimentally reported, while application of non-equilibrium two-phase modeling or pure liquid flow modeling (Bernoulli) would lead to mass flow rates even higher than those predicted by HEM, as already mentioned in the previous section.

A degree of overestimation of the mass flow rate was expected for the same reasons as mentioned in the previous section. It seems though that, a 6 times overestimation is clearly unrealistic and needs to be explained.

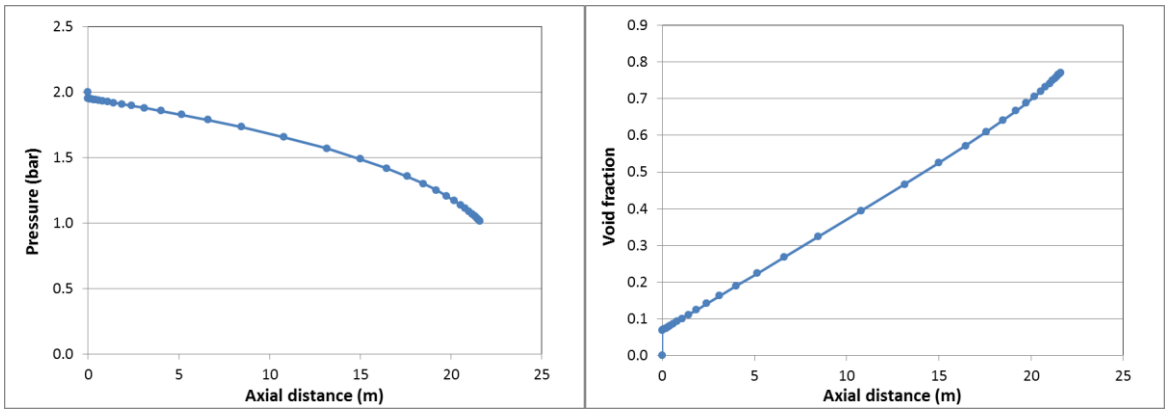

Figure 5. Predicted evolution along discharge line of pressure (left) and void fraction (right), for HSL-2010 tests. Solid circles show the grid locations

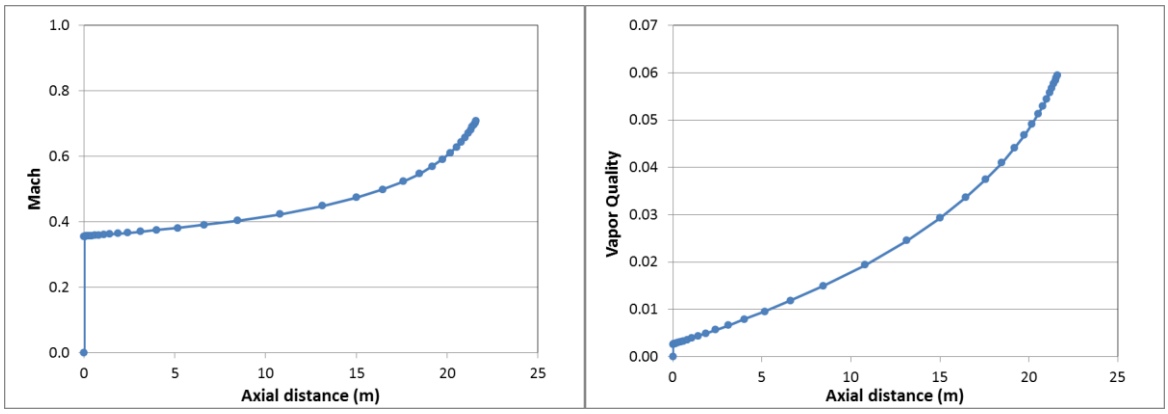

Figure 6. Predicted evolution along discharge line of Mach (left) and vapor quality (right), for HSL-2010 tests. Solid circles show the grid locations

6 CONCLUSIONS AND FUTURE WORK

In this work an engineering computational tool was developed to predict steady state choked flow through a discharge line with variable cross section with account of friction but without wall heat transfer. The tool is able to predict the mass flow rate and the distribution of all relevant physical quantities along the discharge line, even beyond the critical location for both single and two-phase flow.

Focusing on the far more complex two-phase flow, the tool was evaluated against previous experiments with water (relevant to the nuclear industry) and liquefied two-phase hydrogen (relevant to cryogenic hydrogen applications). The relaxation models HRM and DEM were shown to relatively accurately predict the experimental pressure and void fraction distribution along the discharge line for the examined Super Moby Dick water experiment. Due to lack of model coefficients appropriate for hydrogen, only HEM was applied in the case of the LH2 large scale hydrogen release experiments by NASA-1984 and HSL-2010. While predicted mass flow rate for NASA tests was found a factor of 2 above the experimentally reported, a much higher overestimation factor of 6 was the result in case of the HSL tests, both results indicating a) the need for further research on the specific topic and b) the need for much more accurate experiments in terms of mass flow rate estimation.

Future work should focus on: a) further validation of the present computational tool for new hydrogen release experiments (e.g. those to be performed within PRESLHY project) and b) extending the applicability of non-equilibrium models such as HRM and DEM to hydrogen, by finding the corresponding appropriate model coefficients.

7 ACKNOWLEDGEMENTS

The research leading to these results was financially supported by the PRESLHY project, which has received funding from the Fuel Cells and Hydrogen 2 Joint Undertaking under the European Union's Horizon 2020 research and innovation program under grant agreement No 779613.

8 REFERENCES

1. F. D' Auria, and P. Vigni, Two-phase critical flow models, CSNI Report No 49, May 1980, 277 p.
2. G.B. Wallis, Critical two-phase flow. Int. J. Multiphase Flow 6, (1980) 97–112.
3. E. Elias, G.S. Lellouche, Two-phase critical flow. Int. J. Multiphase Flow 20, (1994) 91–168.
4. G.A. Pinhasi, A. Ullmann, A. Dayan, Modelling of flashing two-phase flow. Rev. Chem. Eng. 21, (2005) 133–264.
5. Y. Liao, D. Lucas, Computational modelling of flash boiling flows: A literature survey, International Journal of Heat and Mass Transfer 111 (2017) 246–265.
6. A.G. Venetsanos, Homogeneous non-equilibrium two-phase choked flow modelling, Int. J. of Hydrogen Energy, 43 (50), 22715-22726 (2018).
7. M. De Lorenzo, Ph. Lafon, J.-M. Seynhaeve, Y. Bartosiewicz, Benchmark of Delayed Equilibrium Model (DEM) and classic two-phase critical flow models against experimental data, Int. J. of Multiphase flow, 92 (2017) 112-130.
8. Duponcheel, M. , Seynhaeve, J.-M. , Bartosiewicz, Y. , 2013. Implementation and vali- dation of the DEM model in NEPTUNE_CFD and its application to the simulation of double-choked flows. NURESAFE, report D31.22.12a-b.
9. Z. Bilicki, J. Kestin, M.M. Pratt, A reinterpretation of the results of the Moby Dick experiments in terms on the non-equilibrium model. ASME J. Fluids Eng. 112 (1990) 212–217.
10. P. Downar-Zapolski, Z. Bilicki, L. Bolle, J. Franco, The non-equilibrium relaxation model for one-dimensional flashing liquid flow. Int. J. Multiphase Flow 22 (1996) 473–483.
11. J. W. Leachman, R. T. Jacobsen, S. G. Penoncello, and E. W. Lemmon, "Fundamental Equations of State for Parahydrogen, Normal Hydrogen, and Orthohydrogen," J. Phys. Chem. Ref. Data, 38 (2009) 721-748.
12. W. Wagner…and A. Pruß, The IAPWS Formulation 1995 for the Thermodynamic Properties of Ordinary Water Substance for General and Scientific Use, J. Phys. Chem. Ref. Data, 31 (2002) 387-535.
13. C. Jeandey, L. Gros D'Aillon, R. Bourgine, G. Barriere, Auto vaporisation d' écoulements eau/vapeur. Report TT-163, (1981) CEA, Grenoble.
14. Witcofski R.D., Chirivella J.E., Experimental and analytical analyses of the mechanisms governing the dispersion of flammable clouds formed by liquid hydrogen spills, Int. J Hydrogen Energy 9 (1984) 425–435.
15. P. Hooker, D.B. Willoughby, M. Royle, Experimental releases of liquid hydrogen, 4th Int. Conf. of Hydrogen Safety (ICHS), September 12-14, 2011, San Francisco, US.